EURASIAN PHYSICAL TECHNICAL JOURNAL

2024, Volume 21, No.4 (50)

https://doi.org/10.31489/2024No4/140-148

Received: 04/06/2024 Revised: 13/10/2024 Accepted: 20/12/2024 Published online: 25/12/2024

Original Research Article

UDC 537.533, 535.31

ANALYTICAL DESCRIPTION OF THE POTENTIAL OF ELECTROSTATIC MULTIPOLE SYSTEMS BASED ON A CONDUCTING CIRCULAR CYLINDER

Shugayeva T.Zh.[1], Spivak-Lavrov I.F.[1], Seiten A.B.[1*], Trubitsyn A.A.[2]

[1] Aktobe Regional University named after K. Zhubanov, Aktobe, Kazakhstan
[2] Ryazan State Radio Engineering University named after. V.F. Utkin , Ryazan, Russia
* *Corresponding author*: aizhanat_bolatovna@mail.ru

Abstract. *An urgent task of corpuscular optics and scientific instrumentation is the creation of new methods for calculating the physical and instrumental parameters of mass spectrometers. Leveraging the increased capabilities of computational technology, these methods provide a solid basis for the design and calculation of instruments with improved analytical capabilities. In this work, a method was developed for calculating the electrostatic field of multipole systems based on a conducting circular cylinder. This method uses the broad analytical capabilities of the theory of functions of a complex variable. Analytical expressions are found for the electrostatic field potential of a quadrupole system for the case of infinitely narrow gaps between the electrodes. Analytical expressions for the derivatives of the potential are also obtained. A study was carried out of the influence of the finite size of the gaps between the electrodes on the field configuration. For this purpose, numerical simulations of planar electric fields satisfying the Laplace equation were carried out. The calculation of the electrostatic field potential was carried out using the boundary element method in two stages. First, the distribution of electric charge at the boundary was calculated according to the known boundary potential distribution, that is, the "inverse" problem was solved. Then, using the found values of the charge distribution and the found potential values, the "direct" problem was solved. To solve this problem, a method was developed for solving integral equations with singular and quasi-singular kernels, which provides high accuracy in field calculations for electron-optical systems (EOS) with rectilinear boundaries. The inaccuracies in the calculations resulted solely from rounding mistakes. In the case of an Equation of State characterized by curved boundaries, the precision is dependent exclusively on how accurately the boundaries are represented using linear segments. For the purpose of segmenting the curved borders of the second-order EOS, these boundaries were broken down into arcs with an angular measurement not exceeding one degree.*

Keywords: multipole system, potential, conducting circular cylinder, equipotential lines, anti-resonance system.

1. Introduction

At present, quadrupole mass spectrometers are extensively utilized. This type of mass analyzer is categorized under anti-resonance mass spectrometers, where a portion of the ions is subjected to an electric field comprising both static and oscillating components as they navigate through. In this setup, some ions are able to traverse a specific field with a constrained oscillation amplitude, while the oscillation amplitude for the remaining ions escalates indefinitely over time, causing them to exit the beam [1,2]. The behavior of these charged particles is influenced by their mass-to-charge ratios, enabling the electric field to function as a mass

filter. Consequently, it selectively permits only those ions that possess a designated mass-to-charge ratio to pass through.

The main element of a quadrupole mass analyzer is a linear quadrupole, which is a structure of four cylindrical rods located parallel to each other. Direct and alternating radio frequency voltage is applied to the electrodes.

Quadrupole electrostatic fields are widely used in analytical instrumentation. Quadrupole, sextupole and octupole electrostatic systems are used to correct aberrations of electrostatic lenses and mirrors [3-5]. Quadrupole mass spectrometers, as well as various ion traps that use quadrupole fields, are now widespread. The linear ion trap was proposed by W. Paul in 1952, who was awarded the Nobel Prize in 1989 for these developments [6]. The linear ion trap essentially functions as a quadrupole mass spectrometer, differing primarily due to specific design modifications that allow for stable three-dimensional confinement of charged particles [6-9]. Presently, a variety of linear traps have emerged, including the ion surface trap [10], a microtrap designed for surface studies of a quantum processor [11], and a toroidal ion trap [12]. The fundamental principles of the quadrupole mass spectrometer remain unchanged, despite variations in the spatial configuration and alignment of the electrodes [13]. Furthermore, ion traps hold potential for application in the development of quantum computers [16].

2. Research method

As shown in Fig. 1., a quadrupole electrostatic field is created by setting the potential values $\pm V$ on the surface of a conducting circular cylinder of radius R. In what follows, we will measure linear dimensions in units of R. Thus, a boundary problem arises on the unit circle, the solution of which leads to the Poisson integral for the φ potential [17]:

$$\varphi(\rho,\psi)=\frac{1-\rho^2}{2\pi}\int_0^{2\pi}\frac{V(t)dt}{1+\rho^2-2\rho\cos(t-\psi)}\ . \tag{1}$$

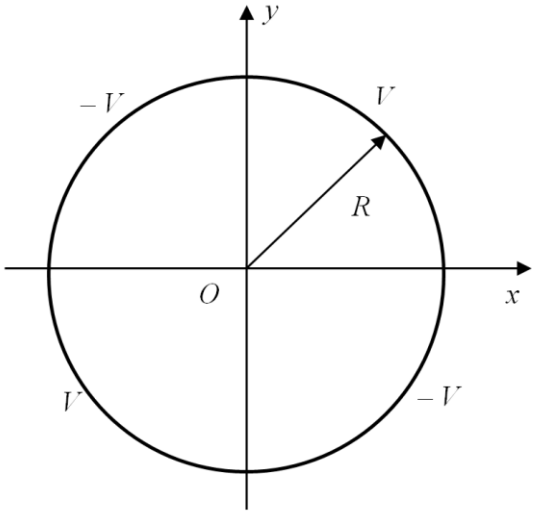

Fig.1. Quadrupole on a cylinder.

Here $V(t)$ – is the angular distribution of potential on the surface of the cylinder.

Let us transform expression (1) to the following form:

$$\varphi(\rho,\psi)=\frac{1-\rho^2}{2\pi}\int_0^{2\pi}\frac{V(t)dt}{1+\rho^2-2\rho(\cos t\cos\psi+\sin t\sin\psi)}\ . \tag{2}$$

To calculate integral (2) we use the following well-known formula:

$$\int\frac{dx}{a+b\cos x+c\sin x}=\frac{2}{\sqrt{a^2-(b^2+c^2)}}\operatorname{arctg}\frac{(a-b)\operatorname{tg}\frac{x}{2}+c}{\sqrt{a^2-(b^2+c^2)}}\ . \tag{3}$$

.

3. Results and discussion

Using formula (3), we write the following expression for potential (2):

$$\varphi(\rho,\psi)=\frac{V}{\pi}\operatorname{arctg}\frac{\left(1+\rho^2+2\rho\cos\psi\right)\operatorname{tg}\frac{t}{2}-2\rho\sin\psi}{1-\rho^2}\Bigg|_0^{\frac{\pi}{2}}-$$

$$-\frac{V}{\pi}\operatorname{arctg}\frac{\left(1+\rho^2+2\rho\cos\psi\right)\operatorname{tg}\frac{t}{2}-2\rho\sin\psi}{1-\rho^2}\Bigg|_{\frac{\pi}{2}}^{\pi^-}+$$

$$\frac{V}{\pi}\operatorname{arctg}\frac{\left(1+\rho^2+2\rho\cos\psi\right)\operatorname{tg}\frac{t}{2}-2\rho\sin\psi}{1-\rho^2}\Bigg|_{\pi^+}^{\frac{3\pi}{2}}-$$

$$-\frac{V}{\pi}\operatorname{arctg}\frac{\left(1+\rho^2+2\rho\cos\psi\right)\operatorname{tg}\frac{t}{2}-2\rho\sin\psi}{1-\rho^2}\Bigg|_{\frac{3\pi}{2}}^{2\pi}. \qquad (4)$$

In cartesian coordinates *x, y, z*, the found potential can be written as:

$$\varphi(x,y)=\frac{2V}{\pi}\left(\operatorname{arctg}\frac{1+\rho^2+2x-2y}{1-\rho^2}-\operatorname{arctg}\frac{1+\rho^2+2x+2y}{1-\rho^2}+\operatorname{arctg}\frac{2y}{1-\rho^2}\right). \qquad (5)$$

Here $\rho=\sqrt{x^2+y^2}$. It is easy to check that, as one would expect, the potential vanishes on the coordinate axes $\varphi(x,0)=\varphi(0,y)=0$. Differentiating expression (3), we find the derivatives of the potential:

$$\frac{\partial\varphi}{\partial x}=\frac{2V}{\pi}\left\{\frac{2\left(1-\rho^2\right)+4x\left(1+x-y\right)}{\left(1-\rho^2\right)^2+\left[1+\rho^2+2\left(x-y\right)\right]^2}-\frac{2\left(1-\rho^2\right)+4x\left(1+x+y\right)}{\left(1-\rho^2\right)^2+\left[1+\rho^2+2\left(x+y\right)\right]^2}+\right.$$

$$\left.+\frac{4xy}{\left(1-\rho^2\right)^2+4y^2}\right\}=V\,f_1(x,y). \qquad (6)$$

$$\frac{\partial\varphi}{\partial y}=\frac{2V}{\pi}\left\{\frac{-2\left(1-\rho^2\right)+4y\left(1+x-y\right)}{\left(1-\rho^2\right)^2+\left[1+\rho^2+2\left(x-y\right)\right]^2}-\frac{2\left(1-\rho^2\right)+4y\left(1+x+y\right)}{\left(1-\rho^2\right)^2+\left[1+\rho^2+2\left(x+y\right)\right]^2}+\right.$$

$$\left.+\frac{2\left(1-\rho^2+2y^2\right)}{\left(1-\rho^2\right)^2+4y^2}\right\}=V\,f_2(x,y). \qquad (7)$$

The derived formulas also characterize the monopole field generated by a segment of a cylindrical electrode at a specific potential, alongside two perpendicular half-planes, xz and yz, which maintain a potential of zero. Figure 2 illustrates the monopole field, depicting equipotential lines at potentials of 0.1V, 0.2V, …, up to 0.9V. These equipotential lines were obtained through the numerical integration of differential equations.

Equipotential lines were found by numerical integration of differential equations:

$$\frac{dy}{dx}=-\frac{\partial\varphi}{\partial x}\Big/\frac{\partial\varphi}{\partial y}\qquad\frac{dx}{dy}=-\frac{\partial\varphi}{\partial y}\Big/\frac{\partial\varphi}{\partial x}. \qquad (8)$$

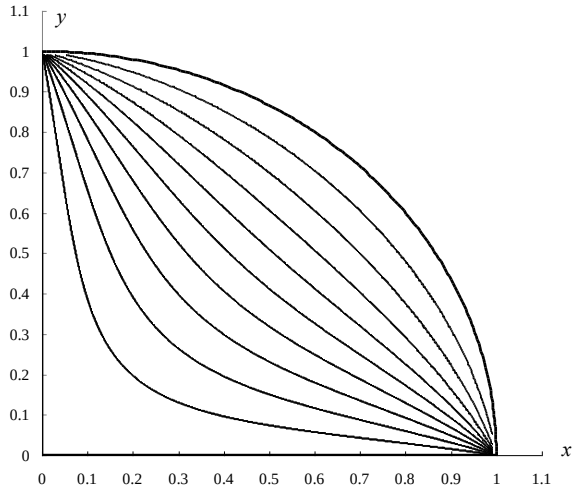

Fig.2. Picture of equipotentials of the field of a cylindrical monopole.

The initial conditions for equations (8) were set on the straight line $y = x$ and according to formula (5) such values were found at which the potential takes the values 0.1 V, 0.2 V, ..., 0.9V. These x values are shown below in Table 1.

Table 1. Values of the x coordinate of equipotential lines on the straight line $y = x$.

φ/V	0.1	0.2	0.3	0.4	0.5	0.6	0.7	0.8	0.9
$x = y$	0.19840	0.28143	0.34648	0.40307	0.45510	0.50475	0.55354	0.60274	0.65348

Using formula (3), we write the following expression for the potential of the sextupole system:

$$\varphi(\rho,\psi)=\frac{V}{\pi}\operatorname{arctg}\frac{\left(1+\rho^2+2\rho\cos\psi\right)\operatorname{tg}\frac{t}{2}-2\rho\sin\psi}{1-\rho^2}\Bigg|_0^{\frac{\pi}{3}}-$$

$$-\frac{V}{\pi}\operatorname{arctg}\frac{\left(1+\rho^2+2\rho\cos\psi\right)\operatorname{tg}\frac{t}{2}-2\rho\sin\psi}{1-\rho^2}\Bigg|_{\frac{\pi}{3}}^{\frac{2\pi}{3}}+$$

$$+\frac{V}{\pi}\operatorname{arctg}\frac{\left(1+\rho^2+2\rho\cos\psi\right)\operatorname{tg}\frac{t}{2}-2\rho\sin\psi}{1-\rho^2}\Bigg|_{\frac{2\pi}{3}}^{\pi}+\ldots\cdot \qquad (9)$$

In Cartesian coordinates x, y, z, the found potential can be written as:

$$\varphi(x,y)=\frac{2V}{\pi}\left(\operatorname{arctg}\frac{2y}{1-\rho^2}+\operatorname{arctg}\frac{\left(1+\rho^2+2x\right)\frac{1}{\sqrt{3}}-2y}{1-\rho^2}-\operatorname{arctg}\frac{\left(1+\rho^2+2x\right)\sqrt{3}-2y}{1-\rho^2}+\right.$$

.

$$-\operatorname{arctg}\frac{\left(1+\rho^2+2x\right)\frac{1}{\sqrt{3}}+2y}{1-\rho^2}+\operatorname{arctg}\frac{\left(1+\rho^2+2x\right)\sqrt{3}+2y}{1-\rho^2}\Bigg). \tag{10}$$

It is easy to check that on the *x* coordinate axis the potential becomes zero $\varphi(x,0)=0$. Now let's find the derivatives of the potential:

$$\frac{\partial\varphi}{\partial x}=\frac{2V}{\pi}\Bigg\{\frac{4xy}{\left(1-\rho^2\right)^2+y^2}+\frac{2\left[(x+1)\frac{1}{\sqrt{3}}\left(1-\rho^2\right)+x\left(1+\rho^2+2x\right)\frac{1}{\sqrt{3}}-2xy\right]}{\left(1-\rho^2\right)^2+\left[\left(1+\rho^2+2x\right)\frac{1}{\sqrt{3}}-2y\right]^2}-$$

$$-\frac{2\left[(x+1)\frac{1}{\sqrt{3}}\left(1-\rho^2\right)+x\left(1+\rho^2+2x\right)\frac{1}{\sqrt{3}}+2xy\right]}{\left(1-\rho^2\right)^2+\left[\left(1+\rho^2+2x\right)\frac{1}{\sqrt{3}}+2y\right]^2}+$$

$$-\frac{2\left[(x+1)\sqrt{3}\left(1-\rho^2\right)+x\left(1+\rho^2+2x\right)\sqrt{3}-2xy\right]}{\left(1-\rho^2\right)^2+\left[\left(1+\rho^2+2x\right)\sqrt{3}-2y\right]^2}+$$

$$+\frac{2\left[(x+1)\sqrt{3}\left(1-\rho^2\right)+x\left(1+\rho^2+2x\right)\sqrt{3}+2xy\right]}{\left(1-\rho^2\right)^2+\left[\left(1+\rho^2+2x\right)\sqrt{3}+2y\right]^2}\Bigg\}=V\,f_1(x,y), \tag{11}$$

$$\frac{\partial\varphi}{\partial y}=\frac{2V}{\pi}\Bigg\{\frac{2\left(1-\rho^2+2y^2\right)}{\left(1-\rho^2\right)^2+4y^2}+\frac{2\left[\left(1-\rho^2\right)\left(\frac{y}{\sqrt{3}}-1\right)+\left(1+\rho^2+2x\right)\frac{y}{\sqrt{3}}-2y^2\right]}{\left(1-\rho^2\right)^2+\left[\left(1+\rho^2+2x\right)\frac{1}{\sqrt{3}}-2y\right]^2}-$$

$$-\frac{2\left[\left(1-\rho^2\right)\left(\frac{y}{\sqrt{3}}+1\right)+\left(1+\rho^2+2x\right)\frac{y}{\sqrt{3}}+2y^2\right]}{\left(1-\rho^2\right)^2+\left[\left(1+\rho^2+2x\right)\frac{1}{\sqrt{3}}+2y\right]^2}-$$

$$-\frac{2\left[\left(1-\rho^2\right)\left(y\sqrt{3}-1\right)+\left(1+\rho^2+2x\right)y\sqrt{3}-2y^2\right]}{\left(1-\rho^2\right)^2+\left[\left(1+\rho^2+2x\right)\sqrt{3}-2y\right]^2}-$$

$$+\frac{2\left[\left(1-\rho^2\right)\left(y\sqrt{3}+1\right)+\left(1+\rho^2+2x\right)y\sqrt{3}+2y^2\right]}{\left(1-\rho^2\right)^2+\left[\left(1+\rho^2+2x\right)\sqrt{3}+2y\right]^2}\Bigg\}=V\,f_2(x,y). \tag{12}$$

We find equipotential lines by numerical integration of differential equations:

$$\frac{dy}{dx}=-\frac{\partial\varphi}{\partial x}\Big/\frac{\partial\varphi}{\partial y},\qquad \frac{dx}{dy}=-\frac{\partial\varphi}{\partial y}\Big/\frac{\partial\varphi}{\partial x}. \tag{13}$$

Table 2. values of the y coordinate equipotential lines on the axis at $x=0$.

φ/V	0.1	0.2	0.3	0.4	0.5	0.6	0.7	0.8	0.9
y/R	0.4285433	0.5410501	0.6215145	0.6874778	0.7454322	0.7987091	0.8493886	0.8989876	0.9487817

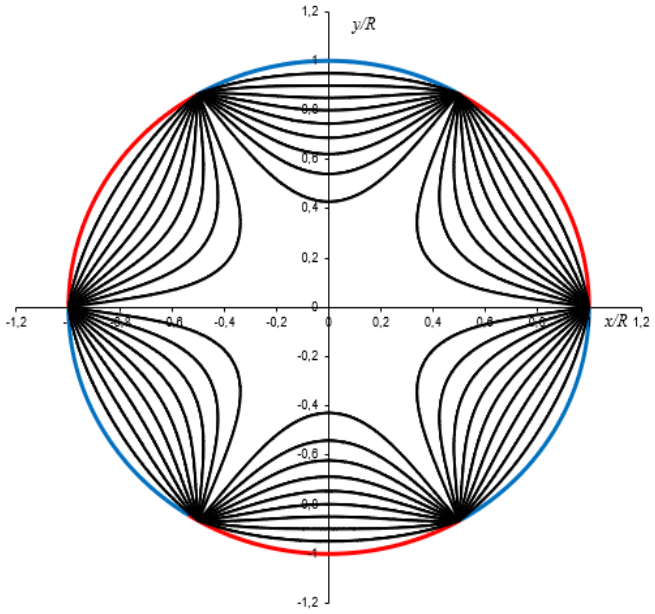

Fig.3. Picture of equipotentials of the field of a cylindrical sextupole.

To confirm the adequacy of the analytical expressions for calculating the electrostatic field proposed in [18], numerical methods for modeling planar electric fields using the boundary element method were used [19].

To tackle the problem numerically, we convert the integral equation that relates the potentials of simple and double layers into a discrete format. This involves dividing the boundary Γ into N boundary elements Γj. By assuming that the potential remains constant along each circuit (electrode) and that the normal derivative of the potential is constant across each boundary element, we can express the integral equation in the following manner:

$$u(\xi)+\sum_{j=1}^{N}u_j H_j(\xi)=\sum_{j=1}^{N}q_j F_j(\xi), \qquad (14)$$

where $\xi\in G\cup\Gamma$ and $\gamma=\pi$ at $\xi\in$G for two-dimensional tasks, $\gamma=2\pi$ at $\xi\in\Gamma$ and $\gamma=4\pi$ at $\xi\in$G for three-dimensional tasks, and the functions $F_j(\xi)$ and $H_j(\xi)$ represent integrals of the fundamental solution and the normal derivative of the fundamental solution of the Laplace equation, respectively [18]. In typical scenarios, these can be computed using standard Gaussian quadrature methods.

The computation of the electrostatic field occurs in two phases. Initially, the unknown vector q_j is derived from the known boundary distribution of the potential $u(\xi\in\Gamma)$ by employing equation (14), effectively addressing the "inverse" problem. Following this, the obtained values of q_j alongside the given u_j are utilized to compute the function $u(\xi)$, for $\xi\in\Omega$ using equation (9), there by resolving the "direct" problem. The author's approach to tackling both inverse and direct problems, as well as the methods for calculating integrals featuring singular and quasi-singular kernels, is thoroughly outlined in the monograph [21].

.

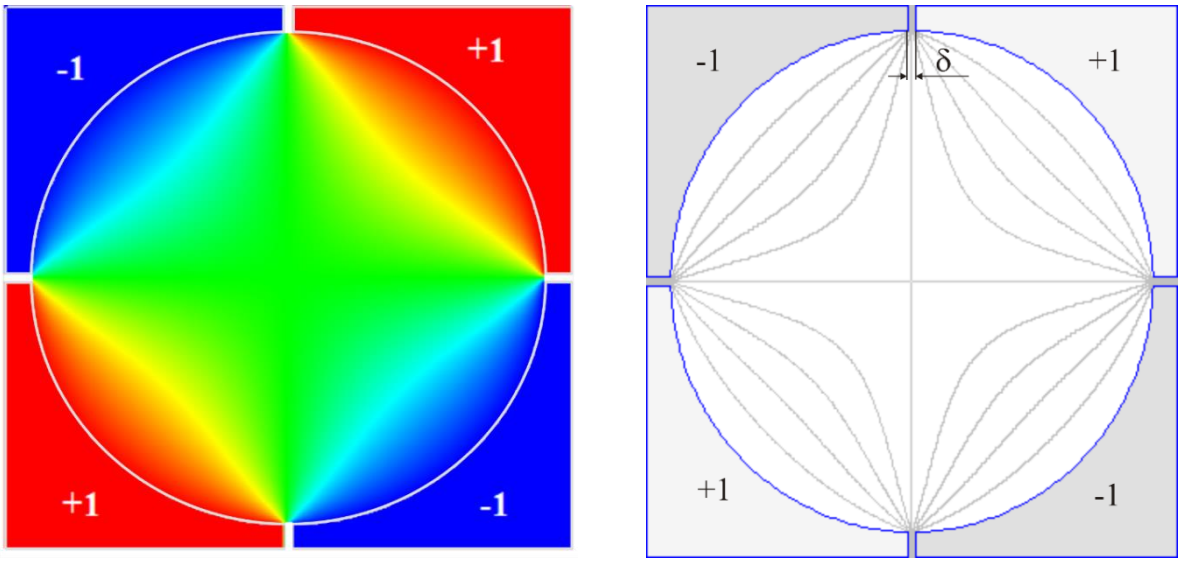

(a) (b)

Fig.4. Two-dimensional potential distribution in a quadrupole system:
a) color coded, b) equipotential lines.

Figure 4 shows the color-coded potential distribution in the internal region of an antiresonant quadrupole system based on a circular conducting cylinder, obtained using the specified numerical technique.

The techniques introduced by the authors [21] for computing integrals in equation (9) involving singular and quasi-singular kernels ensure a high degree of modeling precision. In electron-optical systems (EOS) with straight boundaries, the calculation error is primarily influenced by rounding errors, while for systems with curved boundaries, it is affected by the precision of approximating the boundary using straight line segments.

When segmenting the second-order geometric curves that define the electron-optical systems (EOS) into arcs with a 1° angular increment and approximating these arcs with straight line segments in test scenarios-like a cylindrical capacitor or a quadrupole mass filter featuring hyperbolic electrodes, for which analytical solutions exist-the resulting potential calculation error is found to be no greater than 10^{-3} %.

For the modeled anti-resonance system, when the insulating gap between the electrodes is small and does not exceed the value δ/R=0.1%, the values of the potentials calculated numerically by the boundary element method and by analytical formulas obtained in [18] and in which δ/R=0, also coincide within the error limits of the specified value of 10^{-3} %.

An important fact is the impact of the dimensions of the insulating gap on the deviation of potentials in a quadrupole system from analytically calculated ones, which should be taken into account in the manufacture of real devices. Table 3 presents the results of calculations of potentials along a vertical line located at a certain distance from the origin, which is located at the center of symmetry of the system.

Table 3. Dependence of the potential value in a quadrupole system on *y* at *x/R*=0.1

y/R	0.9	0.8	0.7	0.6	0.5	0.4	0.3	0.2	0.1
δ/*R*=0	0,529976	0,322127	0,22747	0,172661	0,134517	0,103957	0,076791	0,050948	0.025461
δ/*R*=0.2%	0.530	0.3221	0.22747	0.17267	0.13452	0.103965	0.07680	0.050959	0.025474
δ/*R*=3.5%	0.528	0.3216	0.22726	0.17257	0.13446	0.103922	0.07677	0.050928	0.025446
δ/*R*=10%	0.514	0.3173	0.22572	0.17187	0.13408	0.103683	0.07660	0.050822	0.025388

From the analysis of the table data, we can conclude that as we move away from the center and approach the cylindrical boundary of the quadrupole system, the deviation of the potential from the analytical value increases and can exceed 1% with a gap width δ/R=10%; while in the region adjacent to the center of symmetry and which is the working region of the system, the potential deviation does not exceed 0.01%.

4. Conclusion

Using TFCV methods, analytical expressions were obtained for the electrostatic potential of multipole systems based on a conducting circular cylinder for the case of infinitely narrow gaps between the electrodes.

In the considered multipole systems based on a conducting circular cylinder, there is no need to use conducting rods to create a multipole field. The ion beam will move unhindered along the cylinder axis. In this case, we will localize the edge fields using grounded screens at the limits of the system.

The obtained analytical expressions describing the potential distribution in an antiresonance multipole system based on a circular conducting cylinder were tested, and the correctness of the results obtained was confirmed by numerical modeling of the electric field using the boundary element method. The influence of the width of the insulating gap between the electrodes on the magnitude of the potential and on its deviation from the "ideal" one, analytically calculated for the case of an infinitely narrow electrode, has been studied.

Conflict of interest statement

The authors declare that they have no conflict of interest in relation to this research, whether financial, personal, authorship or otherwise, that could affect the research and its results presented in this paper.

CRediT author statement

Spivak-Lavrov I: Conceptualization, Methodology, Supervision ; **Shugayeva T.:** Investigation, Formal Analysis, Writing-Reviewing and Editing ; **Seiten A.:** Writing - original draft, Review and Editing; **Trubitsyn A.:** Software and Analysis. The final manuscript was read and approved by all authors.

Funding

The work was carried out within the framework of a project with grant funding from the Ministry of Science and Higher Education of the Republic of Kazakhstan (AR22685992)

The work was performed as part of the state assignment of the Ministry of Science and Higher Education of the Russian Federation (FSSN-2024-0001)

References

1. Kambarova Z. (2023) Expansion of the functional capacities of electrostatic mirror analyzers for electron spectroscopy. *Eastern-European Journal of Enterprise Technologies*, 5(5(125)), 53–61. DOI: 10.15587/1729-4061.2023.289781.

2. Saulebekov A.O., Kambarova Zh.T., Omarova G.S. (2023) Miniature highly sensitive electron spectrometer for the analysis of corpuscular fluxes. *Eurasian Physical Technical Journal*, 20(2-44), 112–117. DOI: 10.31489/2023NO2/112-117.

3. Preikszas D., Rose H. (1997) Correction properties of electron lenses and mirrors. *Electron microscopy*, 46, 1, 1–9. DOI: 10.1093/oxfordjournals.jmicro.a023484.

4. Szilagyi M. (1990) *Electronic and ion optics*. Moscow, Mir, 639 p. Available at: https://www.libex.ru/detail/book491431.html [in Russian]

5. Hawkes P.W., Spence J.C.H. (2019) *Springer Handbook of Microscopy*, Springer Handbooks, Springer Nature Switzerland AG, 1543 p. DOI: 10.107/978-3-030-00069-1.

6. Paul V. (1990) Electromagnetic traps for charged and neutral particles. *UFN*, 60, 12, 109–127. DOI: 10.3367/UFNr.0160.199012d.0109.

7. Douglas D.J., Frank A.J., Mao D.M. (2005) Linear ion traps in mass spectrometry. *Mass Spectrom. Rev.*, 24 (1), 1–29. DOI: 10.1002/mas.20004.

8. Hager J.W. (2002) A new linear ion trap mass spectrometer. *Rapid Commun. Mass Spectrom.*, 16, 512–526. DOI: 10.1002/rcm.607.

9. March R.E, Todd J.F.J. (2005) *Quadrupole Ion Trap Mass Spectrometry*. Ed. by J.D. Winefordner. Vol. 165., P. 1–78. DOI: 10.1002/0471717983

10. Qiao H., Gao C., Mao D., Konenkov N., Douglas D.J. (2011) Spacecharge effects with mass selective axial ejection from a linear quadrupole ion trap. *Rapid Commun. Mass Spectrom.*, 25, 3509–3520. DOI: 10.1002/rcm.5255.

11. Amini J.M., Britton J., Leibfried D., Wineland D.J. (2011) Microfabricated Chip Traps for Ions Atom Chips. Ed. by J. Reichel, V. Vuletic WILEY-VCH Verlag GmbH & Co.´KGaA, Weinheim. DOI: 10.48550/arXiv.0812.3907.

12. Douglas D.J., Konenkov N.V.(2012) Ion Cloud Model for a Linear Quadrupole Ion Trap. *Euro. J. Mass Spectrom.*, 18, 419–429. DOI: 10.1255/ejms.1200.

13. Douglas D.J., Berdnikov A.S., Konenkov N.V. (2015) The effective potential for ion motion in a radio frequency quadrupole field revisited. *Int. J. Mass Spectrom.*, 377, 345–354. DOI:10.1016/j.ijms.2014.08.009.

14. Rozhdestvensky Yu.V., Rudy S.S. (2017) Linear ion trap with a deterministic voltage of a general form. *Technical Physics*, 87, 4, 625–632. DOI: 10.1134/s1063784217040259.

.

15. Dawson R.H. (1976) *Quadrupole Mass Spectrometry and its Application*, Amsterdam: Elsevier, 1976. Available at: Quadrupole Mass Spectrometry and Its Applications - 1st Edition | Elsevier Shop

16. Baumeester D., Eckert A., Zeilinger A. (2002) *Physics of quantum information*, Moscow: Postmarket, 375 p. Available at: https://www.amazon.com/Physics-Quantum-Information-Cryptography-Teleportation/dp/3540667784

17. Lavrentiev M.A., Shabat B.V. *(*1976) *Methods of the theory of functions of a complex variable*, Moscow: Nauka, 716 p. Available at: https://lib.ysu.am/open_books/93130.pdf

18. Spivak-Lavrov I.F., Shugaeva T.Zh., Seiten A.B. (2023) Anti-resonance quadrupole system based on a circular conducting cylinder. Recent Contributions to Physics, №4 (87), 23-29. DOI:10.26577/RCPh.2023.v87.i4.03. [in Russian]

19. Cheng A. H.-D., Cheng D.T. (2005) Heritage and early history of the boundary element method. *Engineering Analysis with Boundary Elements*, 29, 268–302. DOI: 10.1016/j.enganabound.2004.12.001.

20. Brebbia C.A., Telles J.C.F., Wrobel L.C. (2012) *Boundary Element Techniques: Theory and Applications in Engineering*, London: Springer, 464 p.

21. Gurov V.S., Saulebekov A.O., Trubitsyn A.A. (2015) *Analytical, Approximate-Analytical and Numerical Methods in the Design of Energy Analyzers*, Advances in Imaging and Electron Physics, ed. Peter W. Hawkes, Vol. 192, AIEP, UK: Academic Press, 209 p. DOI: 10.1016/S1076-5670(15)00103-2.

AUTHORS' INFORMATION

Shugayeva, Tilektes Zh. – PhD, K. Zhubanov Aktobe Regional University, Aktobe, Kazakhstan; ORCID iD:0000-0002-4797-4529; tlektes.tleubaeva@gmail.com

Spivak-Lavrov, Igor F. – Doctor of Physical and Mathematical Sciences, Professor, K. Zhubanov Aktobe Regional University, Aktobe, Kazakhstan; ORCID iD: 0000-0001-6235-3897; spivakif@rambler.ru

Seiten, Aizhanat B. – PhD student, K. Zhubanov Aktobe Regional University, Aktobe, Kazakhstan; ORCID iD: 0009-0001-5530-1658; aizhanat_bolatovna@mail.ru

Trubitsyn, Andrey A. – Doctor of Physical and Mathematical Sciences, Professor; Ryazan State Radio Engineering University; Ryazan; Russia; ORCID iD: 0000-0002-9337-8947; assur@bk.ru